Enhanced Energy Transfer within PVK/Alq_3 Polymer Nanowires Induced by the Interface Effect of Nanochannels in Porous Alumina Membrane

Hee-Won Shin, Eun-Jeong Shin, Seung Yeon Cho, Seung-Lim Oh, and Yong-Rok Kim*

Photon Applied Functional Molecule Research Laboratory, Department of Chemistry, Yonsei University, Seoul 120-749, South Korea

Received: May 31, 2007; In Final Form: July 16, 2007

The effect of the interfacial interaction between host−guest materials on energy transfer efficiency was investigated. Porous alumina membrane (PAM) was used as the host, and poly(*N*-vinylcarbazole) (PVK) and tris(8-hydroxyquinoline) aluminum (Alq_3) were guest materials. The energy transfer between PVK and Alq_3 within a PAM shows greatly enhanced efficiency compared with that of the bulk film. Such high efficiency is ascribed to a lowered formation of the fully overlapped form of the PVK excimer, which is induced by strong interaction between the pendant carbazole rings of PVK and the Al centers on the innerchannel surface of the PAM. The photoluminescence lifetimes of PVK become shorter with an increase in the Alq_3 concentration in both films and PAMs, due to the energy transfer. The mean distance between PVK and Alq_3 was estimated by using the Förster formula.

Introduction

Since the first time electroluminescence (EL) in poly(*p*-phenylene vinylene) (PPV) was observed,[1] enormous effort has been given to the investigation of conjugated polymers, because of their potential applications as emitting materials for electroluminescent display.[2−7] The advantages of polymer light-emitting diodes (PLEDs) include fast response times, a simple and cheap solution-based fabrication process, and emission wavelength tunability.[8,9] Particularly, since higher EL efficiency of a PLED is important for its applications, several studies have been performed to improve its EL performance by constructing multilayer devices,[10] removing the imperfections in its chemical and physical structures using thermal annealing,[11] and so on. In addition, it has been revealed that the photophysical property of an emitting polymer is one of the major factors that determine the EL efficiency of the devices, and its efficiency can be improved by using an energy transfer process that causes greater spectral separation between the absorption and the emission (reducing self-absorption).[12,13]

In this paper, we report on the energy transfer process from the hole transport material poly(*N*-vinylcarbazole) (PVK, Scheme 1) to the electron-transporting tris(8-hydroxyquinoline) aluminum (Alq_3) within the morphology of nanowires embedded inside the nanochannels of the porous alumina membrane (PAM) as well as within the bulk film. A PAM, with its well-ordered nanochannel array that is oriented orthogonally to the surface, can be a good candidate for the template for nanopatterned PLEDs, since it provides no quenching factors,[14] possesses thermo- and photostabilities with good mechanical strength,[15] and has uniform pore size and high pore density.[16] Particularly, the confined nanospaces in the pores within the PAM are expected to have an important effect on the changes in the molecular properties of the embedded guest molecules.[17−19]

The energy transfer process from PVK to Alq_3 was investigated by employing steady-state and time-resolved spectroscopies with various Alq_3 doping concentrations. The results indicate that the energy transfer in the PAM system is highly efficient compared with that in the bulk film. The efficiency of energy transfer and the distance between the PVK and Alq_3 in both systems were estimated by using the Förster formula.

SCHEME 1: Chemical Structures of PVK and Alq_3

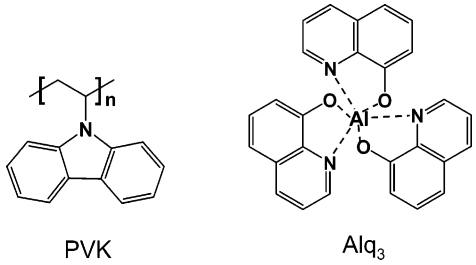

Experimental Section

Materials. The PAM was prepared through a two-step anodizing process of an aluminum plate (99.999%, Aldrich) under a controlled voltage with electrolytes, as reported in the literature.[20] Aluminum foil was anodized, after the annealing and chemical cleaning processes, in a 0.3 M sulfuric acid solution under a constant voltage of 25 V for 20 h. The barrier was removed by chemical etching in a 5 wt % H_3PO_4 aqueous solution for 15 min. The PVK (M_w = 1 100 000 g/mol) and Alq_3 (>95.0%) were purchased from Aldrich and TCI, respectively.

Preparation of PAM Samples. The mixture solutions of the PVK and Alq_3 in dichloromethane were prepared with 0.2, 0.5, and 1 wt % of Alq_3 ratios to the PVK. For the incorporation of the PVK and Alq_3-doped PVK into the nanochannels of the PAM, the empty PAMs were immersed in the solutions for 15 min under ultrasonic conditions. The PAM saturated with the solution was then allowed to be dried at 60 °C for 30 min. Then, the surface of the dried PAM was washed with dichloromethane to remove any polymer residues on the surface. The PAM

* To whom correspondence should be addressed. E-mail: yrkim@yonsei.ac.kr.

10.1021/jp074203m CCC: $37.00
Published on Web 10/02/2007

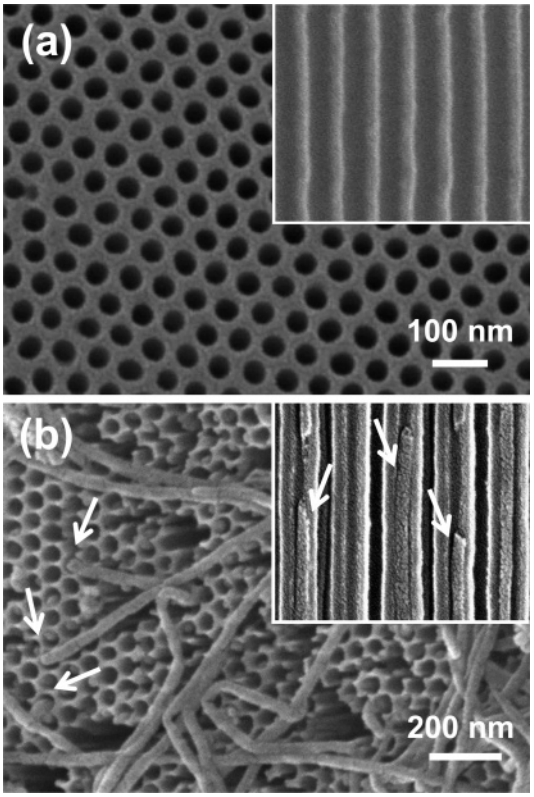

Figure 1. FE-SEM images of top view of (a) the empty PAM (a cross sectional view is shown in the inset) and (b) the partially dissolved PVK−PAM. The arrows indicate the PVK nanowires with a diameter of 40 nm that are arranged to stick out of the nanochannels of the PAM. In the cross sectional view of the PVK−PAM (inset), the arrows indicate the PVK nanowires included in the nanochannels.

samples filled with the PVK and Alq_3-doped PVK are designated as PVK−PAM and Alq_3−PVK−PAM, respectively.

Preparation of Film Samples. As references, the bulk film samples were prepared using the drop-coating method of the above mixture solutions onto quartz plates. The solvent was allowed to evaporate overnight at room temperature.

Spectroscopic Measurements. Steady-state absorption and photoluminescence (PL) spectra were obtained through the use of a diffuse reflectance UV−vis spectrophotometer (JASCO, V-550) equipped with an integrating sphere (JASCO, ISV-469) and a spectrofluorometer (Hitachi, F-4500), respectively. For time-resolved PL studies, all samples were excited with 315 nm picosecond pulses generated from a Raman shifter (18 atm, CH_4) that was pumped by the fourth harmonic pulse (266 nm, fwhm 20 ps, 10 Hz) of a mode-locked Nd:YAG laser (Continuum, Leopard D10). Time-resolved PL spectra and decay data were detected with a picosecond streak camera (Optronis, SCMU-ST-S20) coupled to a spectrometer (CVI, DKSP240) and a CCD system (Optronis, SCRU-SE-S).[21] The typical accumulation number for a PL spectrum was 400 laser shots. Fittings of the PL decays were carried out by a nonlinear least-squares iterative deconvolution method.

Results and Discussion

Characterizations. Morphologies of the PAM samples were characterized by using a field emission scanning electron microscope (FE-SEM, JEOL, JSM-6700F). The typical top view of an empty PAM is shown in Figure 1a, which indicates a hexagonal arrangement of the pores with an average pore diameter of 40 nm. A cross-sectional view (inset in Figure 1a) of the cleaved PAM shows that the nanochannels are straight

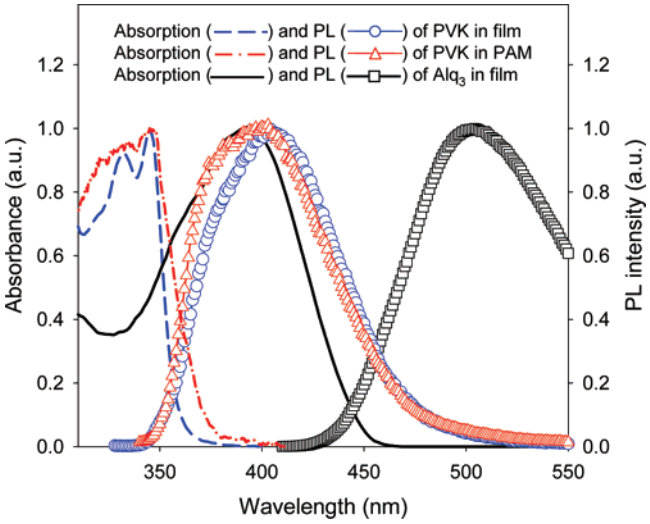

Figure 2. Steady-state absorption and PL spectra of PVK and Alq_3.

and the nanochannel length is about 34 μm. In order to confirm the incorporation of the PVK and Alq_3-doped PVK into the nanochannels of the PAM, the PAM samples were partially dissolved using a 1 M solution of aqueous NaOH. Figure 1b shows the exposed nanowires of the PVK polymer after a partial removal of the PAM: The nanowires with a diameter of 40 nm are arranged to stick out of the nanochannels of the PAM. The inset in Figure 1b is the image of the cleaved cross section of the PVK−PAM, which presents the polymer nanowires filled within the nanochannels of the PAM. This is also confirmed by the Alq_3−PVK−PAM (data not shown).

The thicknesses of the film samples, estimated to be 11−20 μm, were obtained by using a surface profiler (Veeco, Dektak3).

Steady-State Absorption and PL Spectra. The normalized UV−vis absorption and PL spectra of the Alq_3 and PVK are shown in Figure 2. The absorption and PL spectra of the Alq_3 show the peaks at 395 and 505 nm, respectively. The PL spectrum of the PVK film has its maximum at 406 nm. On the other hand, the PL spectrum of the PVK−PAM (λ_{max} = 402 nm) is slightly blue-shifted relative to that of the PVK film, and the shoulder around 375 nm appears to be more distinct for the PVK−PAM than for the PVK film. This behavior is believed to be associated with the interfacial interaction between the innerchannel surface of the PAM and PVK. The origin of this interaction will be discussed in the time-resolved PL section.

The spectral overlap between the emission of the PVK−PAM and the absorption of the Alq_3 appeared to be larger than the overlap between the emission of the PVK film and the absorption of the Alq_3, as shown in Figure 2. To understand the effect of the spectral overlap on the energy transfer, the Förster radius (R_0) can be derived from the overlap of the donor emission and acceptor absorption spectra, as demonstrated in the Förster energy transfer theory.[22]

$$R_0^{\,6} = \frac{9000(\ln 10)\kappa^2\varphi_d}{128\pi^5 N n^4} J \qquad (1)$$

where

$$J = \int F_d(\lambda)\,\epsilon_a(\lambda)\lambda^4\,d\lambda$$

and κ^2 (0−4; $^2/_3$ for randomly oriented dipoles) is a factor describing the orientation of the transition dipoles of a donor relative to that of an acceptor, φ_d is the fluorescence quantum yield of the donor in the absence of acceptor, J is the overlap

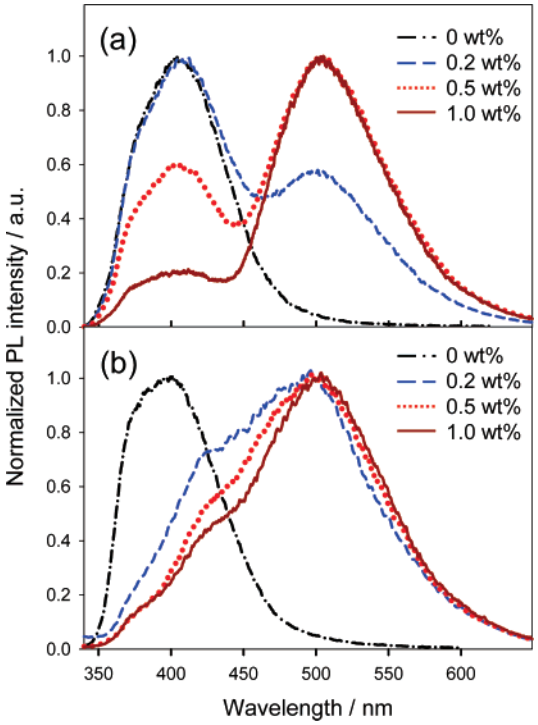

Figure 3. Normalized PL spectra of (a) Alq_3-doped PVK films and (b) Alq_3−PVK−PAMs with different Alq_3 doping concentrations. Excitation wavelength for all PL spectra was 315 nm.

TABLE 1: PL Intensity Ratio (I_{505nm}/I_{370nm}) in the Alq_3-Doped PVK Films and the Alq_3−PVK−PAMs[a]

Alq_3 concn (wt %)	I_{505nm}/I_{370nm} in film	I_{505nm}/I_{370nm} in PAM
0.2	1.0	5.3
0.5	2.6	8.8
1.0	7.4	9.3

[a] The excitation wavelength was 315 nm.

integral, N is Avogadro's number, n is the refractive index of the medium, $F_d(\lambda)$ is the fluorescence intensity of the donor at wavelength (nm), and $\epsilon_a(\lambda)$ is the molar extinction coefficient of the acceptor. Assuming that the value of $\kappa^2 = {}^2/_3$, it is evaluated that the value of R_0 in the PAM (38.9 Å) is slightly larger than that in the film (38.2 Å). This means that the energy transfer process from the PVK to the Alq_3 is expected to be more efficient in the PAM system than in film.

To test the energy transfer, film and PAM samples with different Alq_3 doping concentrations were prepared and optically excited with 315 nm. Figure 3 presents the normalized PL spectra of the Alq_3-doped PVK films and the Alq_3−PVK−PAMs. As the Alq_3 concentration increases, the Alq_3 emission around 505 nm gradually grows at the expense of the PVK emissions, in both the Alq_3-doped PVK films and in the Alq_3−PVK−PAMs. Particularly, at a low Alq_3 concentration of 0.2 wt %, it is noted that the quenching of the PVK emission is greatly enhanced in the Alq_3−PVK−PAM.

The PL intensity ratio of Alq_3 (I_{505nm}) to PVK (I_{370mn}) denotes the extent of energy transfer from PVK to Alq_3. From Table 1, the values of the ratios in Alq_3−PVK−PAMs are larger than those of Alq_3-doped PVK films. The ratio at a low Alq_3 concentration noticeably shows the 5 times difference between the values of the Alq_3-doped PVK film and Alq_3−PVK−PAM.

Time-Resolved PL Spectra and Decay Profiles. To obtain dynamic information concerning the excited states and the energy transfer process, picosecond transient PL spectra were measured. Figure 4 presents the streak camera images (inset in the upper right side) and the time-resolved PL spectra of the Alq_3-doped PVK films and the Alq_3−PVK−PAMs with different doping concentrations. In pure PVK film (Figure 4a), at an early gate-time, the PL spectrum shows a maximum of 385 nm with a shoulder around 365 nm. Then, the PL maximum is subsequently shifted to the longer wavelength of 420 nm, as the gate-time is delayed. Such spectral characteristics are due to the excited-state energy distribution among the emitting species of the monomer and other excimers which are generalized into two types. One is a fully overlapped structure between the two neighboring carbazole groups (denoted as a full overlap excimer) and the other is a partially overlapped structure between the two groups (denoted as a partial overlap excimer).[23] A previous study done in degassed THF solution stated that the PLs of the monomer ($\lambda_{max} \approx 350$ nm) and the partial overlap excimer ($\lambda_{max} \approx 370$ nm) were observed immediately after a photoexcitation, while that of the full overlap excimer ($\lambda_{max} \approx 420$ nm) predominantly appeared at a late gate-time,[24] which is generally consistent with the data obtained in our study.

The temporal evolution of the PL spectra of the PVK−PAM (Figure 4e) is comparable to that of the PVK film (Figure 4a). However, the evolutions of the PL spectra for the Alq_3−PVK−PAMs (Figure 4f−h) are remarkably different from those of the Alq_3-doped PVK films (Figure 4b−d). Even at an early time, the Alq_3 emissions are very intensive compared with the relatively weak PVK emissions in the 0.2−1.0 wt % Alq_3−PVK−PAM (Figure 4f−h).

Figure 5 shows typical PL decay curves at different detection wavelengths. The fitted PL lifetimes and their relative amplitudes are listed in Tables 2 and 3. The PL decay curve of the PVK film exhibits double-exponential decay components at the detection wavelength of 370 nm, which corresponds to the emission wavelengths of the monomer and the partial overlap excimer. At 420 nm, the PL decay curve appears to exhibit triple-exponential components due to the inclusion of the emission state of the full overlap excimer. According to Sakai et al., the monomer lifetime is the shortest due to its efficient energy transfer to the excimers, and the lifetime of the full overlap excimer is the longest.[24] Therefore, the PL lifetimes of the monomer (τ_1) and the partial and full overlap excimers (τ_2 and τ_3) are assigned as 0.30, 1.3, and 7.8 ns, respectively.

From Table 2, the PL lifetimes (τ_1 and τ_2) of the PVK decrease with an increase in the Alq_3 concentration due to the energy transfer from the PVK to the Alq_3. The point to note here is that the rise components at 560 nm that correspond to the Alq_3 emission are observed to be significant at the Alq_3 doping concentrations of 0.5 wt % (0.86 ns) and 1.0 wt % (0.77 ns). Since the energy transfer mainly depends on the spectral overlap between the emission of a donor and the absorption of an acceptor,[22] it is considered that the monomer and the partial overlap excimer of the PVK are preferable to the energy transfer to the Alq_3, because of their larger spectral overlaps with the Alq_3 absorption than the case of the full overlap excimer. With a low acceptor concentration (0.2 wt % Alq_3), the major contributions to the energy transfer are expected to be from the monomer and the partial overlap excimer, which results in the buildup of the Alq_3 emission faster than our detection limit (~20 ps). However, with high acceptor concentrations (0.5 and 1.0 wt %), the Alq_3 can be excited by not only the efficient energy transfer from the monomer and the partial overlap excimer but also the less favorable energy transfer from the full overlap excimer. Therefore, the origin of the observed rise components

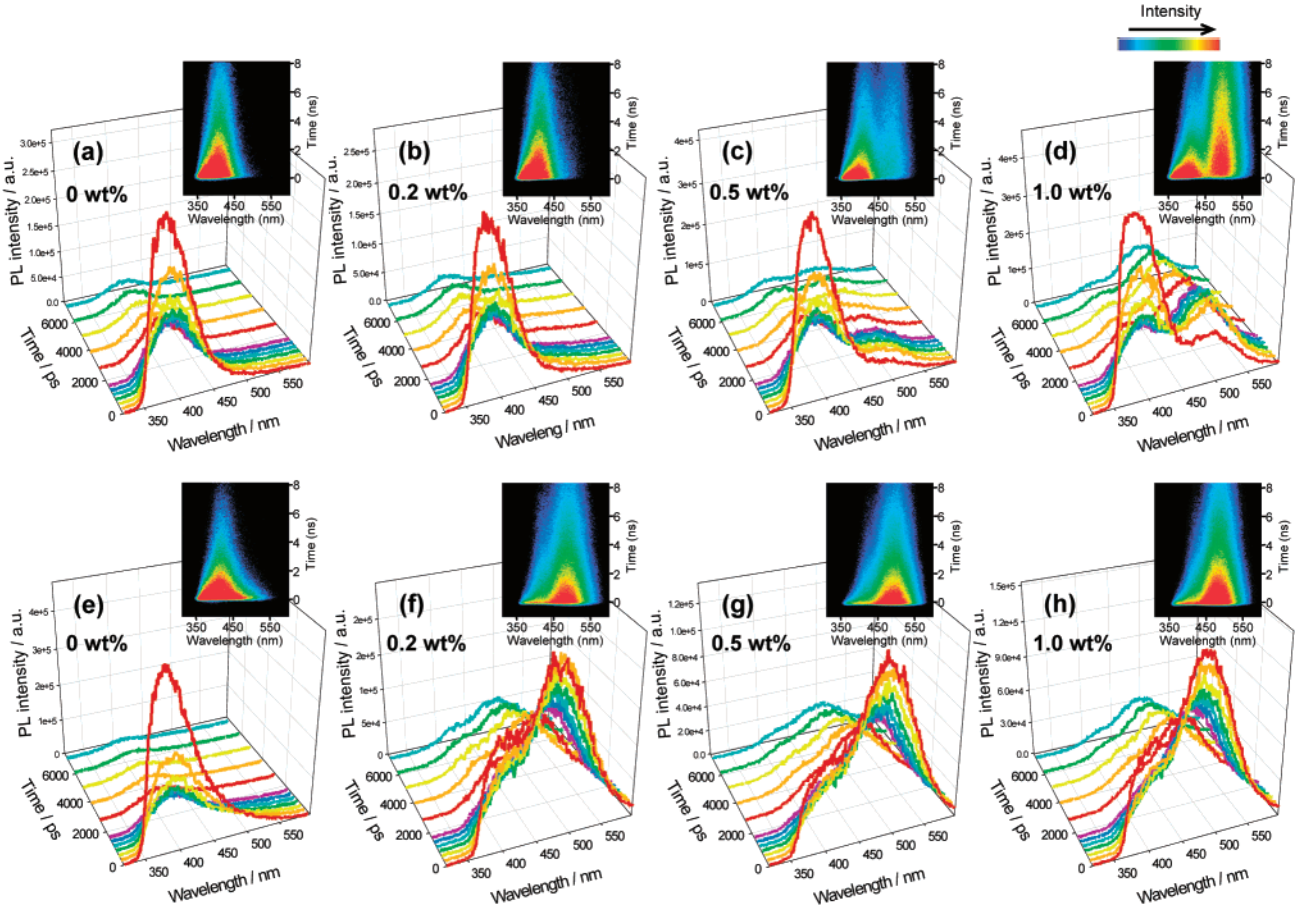

Figure 4. Time-resolved PL spectra of Alq_3-doped PVK films (a−d) and Alq_3−PVK−PAMs (e−h) with different Alq_3 doping concentrations. Streak camera images are shown in insets.

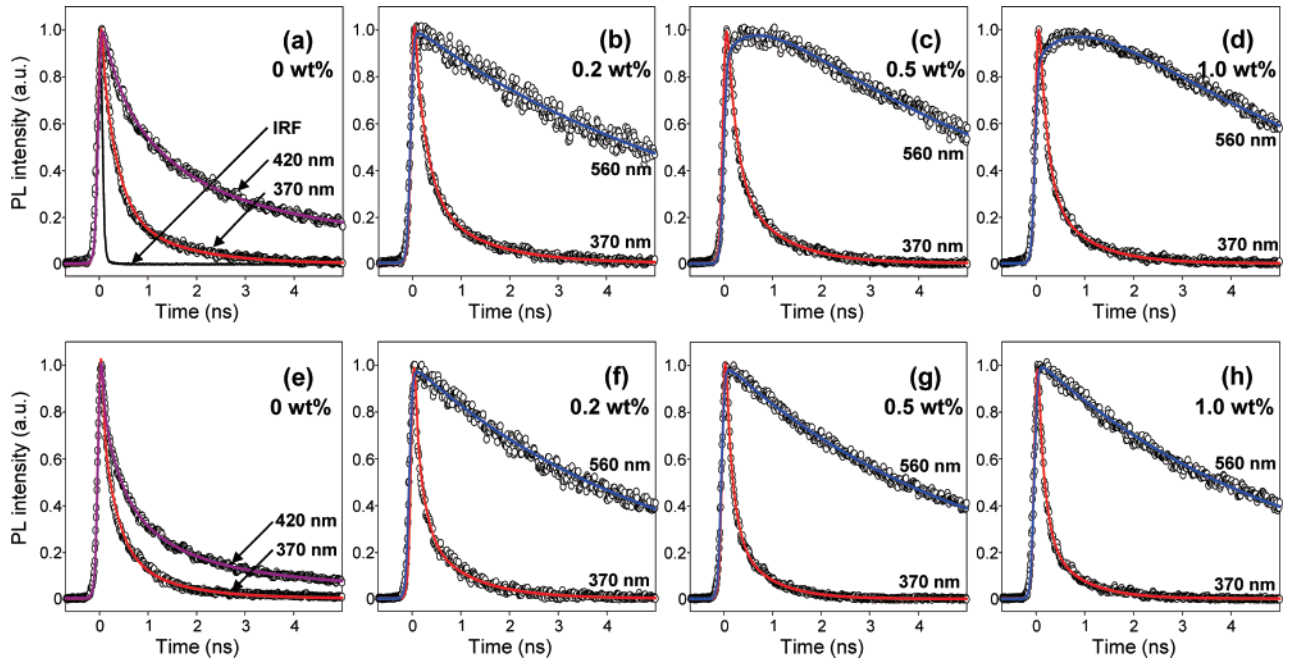

Figure 5. Typical PL decay profiles of Alq_3-doped PVK films (a−d) and Alq_3−PVK−PAMs (e−h) with different Alq_3 doping concentrations at several detection wavelengths. Solid lines along the data points are fitted lines. IRF denotes instrument response function.

is attributed to a less favorable energy transfer from the full overlap excimer. The faster rise time upon increasing the Alq_3 concentration (from 0.5 to 1.0 wt %) can be explained by the Förster energy transfer theory.[22,25]

In the PAM systems, although the PL lifetimes of the monomer and both of the excimers in the PVK−PAM are comparable to those in the PVK film, the emission amplitude ratios of the monomer and both of the excimers are significantly different from those in the film. The PL decay curve of the PVK−PAM appears to be much faster than that of the PVK film at 420 nm, although the PL decay curves at 370 nm are similar for both (see Figure 5a,e). This suggests that the

TABLE 2: PL Lifetimes (τ) and Their Relative Amplitudes (A) of Pure PVK and Alq_3-Doped PVK Films[a]

		PVK				Alq_3	
Alq_3 (wt %)	λ (nm)	decay τ_1 (ns)/A_1	decay τ_2 (ns)/A_2	decay τ_3 (ns)/A_3	$\langle\tau\rangle^b$	rise τ_1 (ns)	decay τ_2(ns)
0	370	0.30/0.74	1.3/0.26		0.55		
	420	0.30/0.24	1.3/0.48	7.8/0.28	2.9		
0.2	370	0.25/0.72	1.2/0.28		0.50		
	560						5.9
0.5	370	0.18/0.71	0.91/0.29		0.40		
	560					0.86	6.1
1.0	370	0.16/0.74	0.83/0.26		0.33		
	560					0.77	6.2

[a] The excitation wavelength for all decays was 315 nm. [b] The weighted average lifetime, which is defined as $\sum A_i\tau_i/\sum A_i$. The parameters are estimated from iterative least-squares deconvolution fitting of the emission decays with the expression $I(t) = A_1 \exp(-t/\tau_1) + A_2 \exp(-t/\tau_2) + A_3 \exp(-t/\tau_3)$; $I(t)$, A, and τ are the time-dependent PL intensity, relative amplitude, and lifetime, respectively.

TABLE 3: PL Lifetimes (τ) and Their Relative Amplitudes (A) of PVK−PAM and Alq_3−PVK−PAM[a]

		PVK				Alq_3
Alq_3 (wt %)	λ (nm)	decay τ_1 (ns)/A_1	decay τ_2 (ns)/A_2	decay τ_3 (ns)/A_3	$\langle\tau\rangle^b$	decay τ (ns)
0	370	0.29/0.72	1.1/0.28		0.52	
	420	0.30/0.44	1.2/0.43	7.8/0.13	1.7	
0.2	370	0.16/0.71	0.96/0.29		0.39	
	560					5.8
0.5	370	0.14/0.73	0.72/0.27		0.30	
	560					5.9
1.0	370	0.13/0.75	0.72/0.25		0.28	
	560					5.9

[a] The excitation wavelength for all decays was 315 nm. [b] The weighted average lifetime which is defined as $\sum A_i\tau_i/\sum A_i$. The parameters are estimated from iterative least-squares deconvolution fitting of the emission decays with the expression $I(t) = A_1 \exp(-t/\tau_1) + A_2 \exp(-t/\tau_2) + A_3 \exp(-t/\tau_3)$; $I(t)$, A, and τ are the time-dependent PL intensity, relative amplitude, and lifetime, respectively.

monomers and the partial overlap excimers exist more abundantly in the PAM than in the film. In the case of a nanoporous host−guest system, a large interfacial area and a confined environment may affect the intermolecular forces between the host and the guest, thus leading to a significant change in the molecular property of the embedded guest.[18,19,26,27] Previous reports state that the conjugated polymers containing aromatic rings can be adsorbed onto the innerchannel surface of the PAM through the interaction between the aromatic rings and the Al centers on the surface of the PAM.[17,28,29] Therefore, it is expected that the interaction between the Al centers on the innerchannel surface of the PAM and the pendant carbazole rings of the PVK restrict the rotational motion of carbon−carbon bonds in the PVK chains. Such restriction of the rotational motion results in the formation of fewer full overlap excimers that require the rotation of the neighboring carbazole group to maintain a face-to-face structure. Note that the blue shift in the PL spectrum of the PVK−PAM (Figure 2) is ascribed to the increased portion of monomers and partial overlap excimers as compared to full overlap excimers.

In the Alq_3−PVK−PAMs, although the PL lifetimes of the PVK became shorter with increasing Alq_3 concentration, a rise in the Alq_3 emission was not observed in our detection resolution limit (Table 3). This is because the energy transfer to the Alq_3 takes place mainly via an efficient pathway from the monomer and the partial overlap excimer, even at high Alq_3 concentrations (0.5 and 1.0 wt %).

Energy Transfer Efficiency and Distance between PVK and Alq_3. To evaluate the efficiency of energy transfer (E), the weighted average lifetime ($\langle\tau\rangle$) is applied. E can be determined by the extent of donor quenching due to the acceptor from eq 2, where τ_d and τ_{da} are the PL lifetimes of the donors in the absence and presence of acceptors, respectively.[22]

$$E = 1 - \frac{\tau_{da}}{\tau_d} \tag{2}$$

From Tables 2 and 3, it can be seen that $\langle\tau\rangle$ of the PVK film is 0.55 ns, while for the Alq_3-doped PVK film with 0.2, 0.5, and 1.0 wt %, it is 0.50, 0.40, and 0.33 ns, respectively. In the case of the PAM system, $\langle\tau\rangle$ without the Alq_3 is 0.52 ns, while for Alq_3 concentrations of 0.2, 0.5, and 1.0 wt %, it is 0.39, 0.30, and 0.28 ns, respectively. On the basis of the observed lifetimes, eq 2 yields that the energy transfer efficiencies are 0.07, 0.27, and 0.40 for the Alq_3-doped films, and 0.24, 0.43, and 0.46 for the Alq_3−PVK−PAMs, with Alq_3 concentrations of 0.2, 0.5, and 1.0 wt %, respectively. Therefore, it suggests that the Alq_3−PVK−PAM systems show greatly enhanced energy transfer efficiencies compared with those of the bulk films.

Also, the energy transfer efficiency can be represented as the fraction of the Förster radius and the mean distance (R) between the donor and the acceptor.[22] The efficiency decreases as R becomes larger above R_0, while it approaches 1.0 as R becomes much smaller than R_0.

$$E = \frac{{R_0}^6}{{R_0}^6 + R^6} \tag{3}$$

Using eqs 1−3, the mean distances between the PVK and the Alq_3 were calculated to be 58.8, 45.1, and 40.1 Å for the Alq_3-doped films, and 47.1, 40.8, and 39.9 Å for the Alq_3−PVK−PAMs, with Alq_3 concentrations of 0.2, 0.5, and 1.0 wt %, respectively. The R decreases with increasing Alq_3 concen-

tration in both systems. Because of the monomer and partial overlap excimer, which are induced more within the PAM system, the mean distance is significantly shorter in the PAM than the film at the same concentrations of PVK and Alq_3 in both systems.

Conclusions

The resonance energy transfer efficiency is greatly enhanced in the Alq_3−PVK−PAM systems in comparison to the Alq_3-doped PVK films. The enhanced energy transfer efficiency in the nanochannel environment of the PAM is attributed to the large spectral overlap caused by the less pronounced formation of the full overlap excimers. This is due to the strong interaction between the PVK and the alumina surface within the nanochannels of the PAM. We believe that a nanochannel system that provides high energy transfer efficiency can be utilized in the fabrication of highly efficient PLED.

Acknowledgment. This work was supported by the Korea Science and Engineering Foundation (KOSEF) through the National Research Lab. Program funded by the Ministry of Science and Technology (No. R0A-2003-000-10305-0) and Seoul R&BD Program (10816). H.-W.S. and S.-L.O. thank the fellowship of the BK 21 program from the Ministry of Education and Human Resources Development.

References and Notes

(1) Burroughes, J. H.; Bradley, D. D. C.; Brown, A. R.; Marks, R. N.; Mackay, K.; Friend, R. H.; Burns, P. L.; Holmes, A. B. *Nature* **1990**, *347*, 539.

(2) Salaneck, W. P.; Lundstorm, I.; Ranby, B. *Conjugated Polymers and Related Materials*; Oxford University Press: Oxford, 1993; pp 65−169.

(3) Braun, D.; Heeger, A. J. *Appl. Phys. Lett.* **1991**, *58*, 1982.

(4) Chung, S.-J.; Kwon, K.-Y.; Lee, S.-W.; Jin, J.-I.; Lee, C. H.; Lee, C. E.; Park, Y. *Adv. Mater.* **1998**, *10*, 1112.

(5) Friend, R. H.; Gymer, R. W.; Holmes, A. B.; Burroughes, J. H.; Marks, R. N.; Taliani, C.; Bradley, D. D. C.; Dos Santos, D. A.; Brédas, J. L.; Lögdlund, M.; Salaneck, W. R. *Nature* **1999**, *397*, 121.

(6) Cheon, C. H.; Joo, S.-H.; Kim, K.; Jin, J.-I.; Shin, H.-W.; Kim, Y.-R. *Macromolecules* **2005**, *38*, 6336.

(7) Al Attar, H. A.; Monkman, A. P.; Tavasli, M.; Bettington, S.; Bryce, M. R. *Appl. Phys. Lett.* **2005**, *86*, 121101.

(8) List, E. J. W.; Tasch, S.; Hochfilzer, C.; Leising, G.; Schlichting, P.; Rohr, U.; Geerts, Y.; Scherf, U.; Müllen, K. *Opt. Mater.* **1998**, *9*, 183.

(9) Cerullo, G.; Stagira, S.; Zavelani-Rossi, M.; Silvestri, S. D.; Virgili, T.; Lidzey, D. G.; Bradley, D. D. C. *Chem. Phys. Lett.* **2001**, *335*, 27.

(10) Bradley, D. D. C. *Synth. Met.* **1993**, *54*, 401.

(11) Chou, H.-L.; Lin, K.-F.; Fan, Y.-L.; Wang, D.-C. *J. Polym. Sci., Part B: Polym. Phys.* **2005**, *43*, 1705.

(12) Peng, K.-Y.; Chen, S.-A.; Fann, W.-S. *J. Am. Chem. Soc.* **2001**, *123*, 11388.

(13) Gong, X.; Ostrowski, J. C.; Moses, D.; Bazan, G. C.; Heeger, A. J. *Adv. Funct. Mater.* **2003**, *13*, 439.

(14) Kukhta, A. V.; Gorokh, G. G.; Kolesnik, E. E.; Mitkovets, A. I.; Taoubi, M. I.; Koshin, Y. A.; Mozalev, A. M. *Surf. Sci.* **2002**, *507*−*510*, 593.

(15) Li, Y.; Meng, G. W.; Zhang, L. D.; Phillipp, F. *Appl. Phys. Lett.* **2000**, *76*, 2011.

(16) Shin, H.-W.; Cho, S.-Y.; Choi, K.-H.; Oh, S.-L.; Kim, Y.-R. *Appl. Phys. Lett.* **2006**, *88*, 263112.

(17) Qi, D.; Kwong, K.; Rademacher, K.; Wolf, M. O.; Young, J. F. *Nano Lett.* **2003**, *3*, 1265.

(18) Park, J.-W.; Chae, W.-S.; Shin, H.-W.; Kim, Y.-R.; Lee, J.-K. *Mol. Cryst. Liq. Cryst.* **2005**, *432*, 59.

(19) Steinhart, M.; Zimmermann, S.; Göring, P.; Schaper, A. K.; Gösele, U.; Weder, C.; Wendorff, J. H. *Nano Lett.* **2005**, *5*, 429.

(20) Masuda, H.; Satoh, M. *Jpn. J. Appl. Phys.* **1996**, *35*, L126.

(21) Chae, W.-S.; Shin, H.-W.; Lee, E.-S.; Shin, E.-J.; Jung, J.-S.; Kim, Y.-R. *J. Phys. Chem. B* **2005**, *109*, 6204.

(22) Lakowicz, J. R. *Principles of Fluorescence Spectroscopy*; Plenum Press: New York, 1983; pp 303−339.

(23) Itaya, A.; Okamoto, K.; Kusabayashi, S. *Bull. Chem. Soc. Jpn.* **1976**, *49*, 2082.

(24) Sakai, H.; Itaya, A.; Masuhara, H.; Sasaki, K.; Kawata, S. *Polymer* **1996**, *37*, 31.

(25) Lutkouskaya, K.; Calzaferri, G. *J. Phys. Chem. B* **2006**, *110*, 5633.

(26) Márquez, F.; García, H.; Palomares, E.; Fernández, L.; Corma, A. *J. Am. Chem. Soc.* **2000**, *122*, 6520.

(27) Scott, B. J.; Wirnsberger, G.; Stucky, G. D. *Chem. Mater.* **2001**, *13*, 3140.

(28) Tirendi, C. F.; Mills, G. A.; Dybowski, C. R. *J. Phys. Chem.* **1989**, *93*, 3282.

(29) Vanderbeek, G. P.; Stuart, M. A. C.; Fleer, G. J.; Hofman, J. E. *Macromolecules* **1991**, *24*, 6600.